UC-34A
LBL-20835
c.1

Lawrence Berkeley Laboratory

UNIVERSITY OF CALIFORNIA

RECEIVED
LAWRENCE
BERKELEY LABORATORY
MAR 6 1986
LIBRARY AND
DOCUMENTS SECTION

Accelerator & Fusion Research Division

Presented at the Synchrotron Radiation Sources
and Their Applications Conference,
Aberdeen, Scotland, September 14-18, 1985

MONOCHROMATOR SYSTEMS

M.R. Howells

December 1985

For Reference

Not to be taken from this room

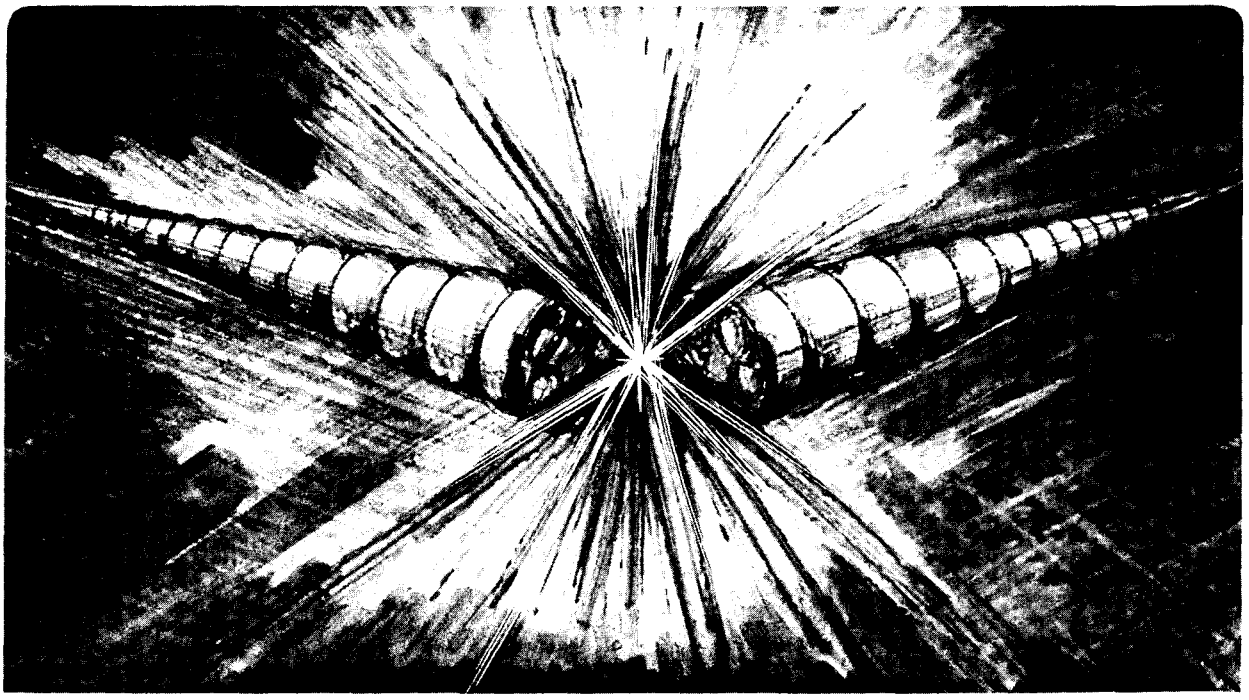

LBL-20835
c.1

Prepared for the U.S. Department of Energy under Contract DE-AC03-76SF00098

DISCLAIMER

This document was prepared as an account of work sponsored by the United States Government. While this document is believed to contain correct information, neither the United States Government nor any agency thereof, nor the Regents of the University of California, nor any of their employees, makes any warranty, express or implied, or assumes any legal responsibility for the accuracy, completeness, or usefulness of any information, apparatus, product, or process disclosed, or represents that its use would not infringe privately owned rights. Reference herein to any specific commercial product, process, or service by its trade name, trademark, manufacturer, or otherwise, does not necessarily constitute or imply its endorsement, recommendation, or favoring by the United States Government or any agency thereof, or the Regents of the University of California. The views and opinions of authors expressed herein do not necessarily state or reflect those of the United States Government or any agency thereof or the Regents of the University of California.

MONOCHROMATOR SYSTEMS

LECTURE 3:

Malcolm R. Howells
Center for X-ray Optics, Lawrence Berkeley Laboratory
1 Cyclotron Road, Berkeley, California 94720

1. INTRODUCTION

We discuss general properties of monochromators and give some useful formulas for optical design. We do not have space to discuss particular instruments but we give fairly comprehensive references. An excellent comprehensive review is given by Johnson.[24]

2. DIFFRACTION GRATINGS

We consider only the most useful type of grating which is a Rowland reflection grating. The groove pattern consists of the intersection of the substrate surface with a set of parallel equispaced planes. The notation for dealing with it is shown in fig 1. The basic relationship between the angles of incidence (α) and diffraction (β) is:

$$m\lambda = d(\sin\alpha + \sin\beta), \qquad (1)$$

where λ is the wavelength. α and β have opposite signs if they are on opposite sides of the normal. Apparently there are an infinite number of α,β pairs corresponding to any given λ. Therefore, we are free to impose a relationship between α and β. The following relationships are used:

2.1 The on-blaze condition

For a saw tooth grating with angle θ_B we can require that the diffracted ray be formed by a specular reflection off the blaze facet. In this case

$$\alpha + \beta = 2\theta_B \qquad (2)$$

Eliminating α between (1) and (2) gives

$$m\lambda = 2d\sin\theta_B \cos(\beta+\theta_B) \qquad (3)$$

Notice that (3) is the Bragg condition for the blaze facets as Bragg

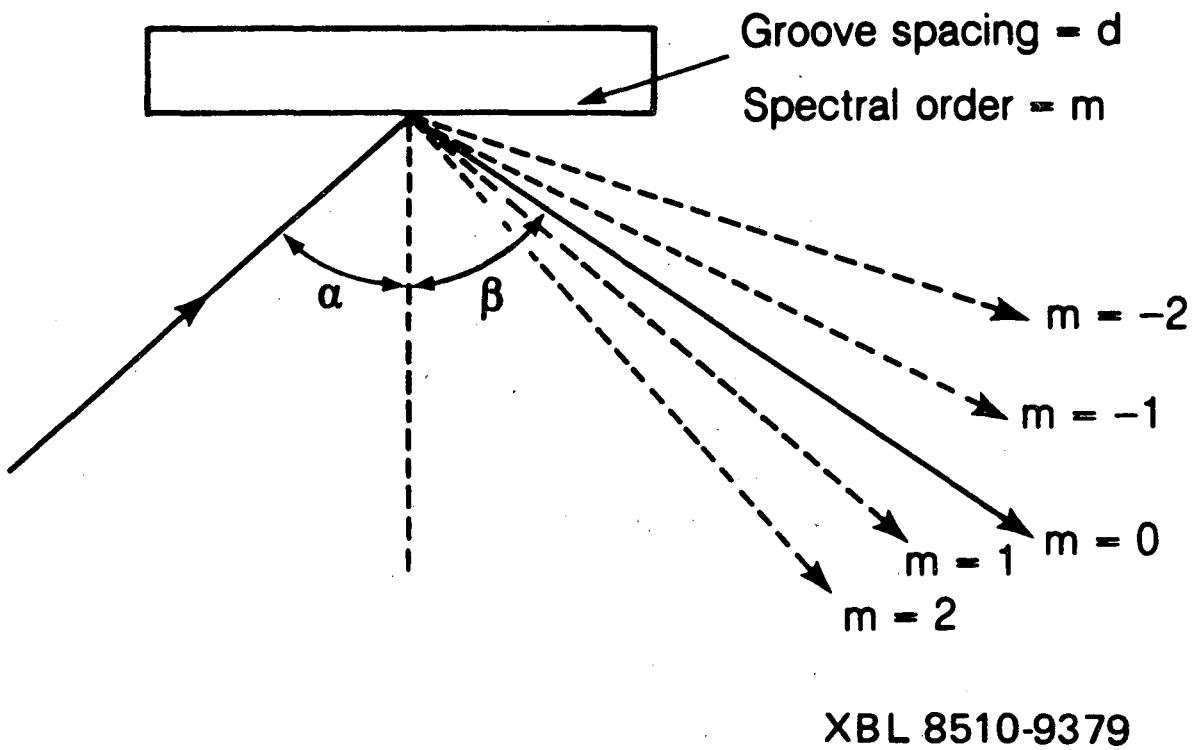

Fig. 1 Notation for diffraction by a grating

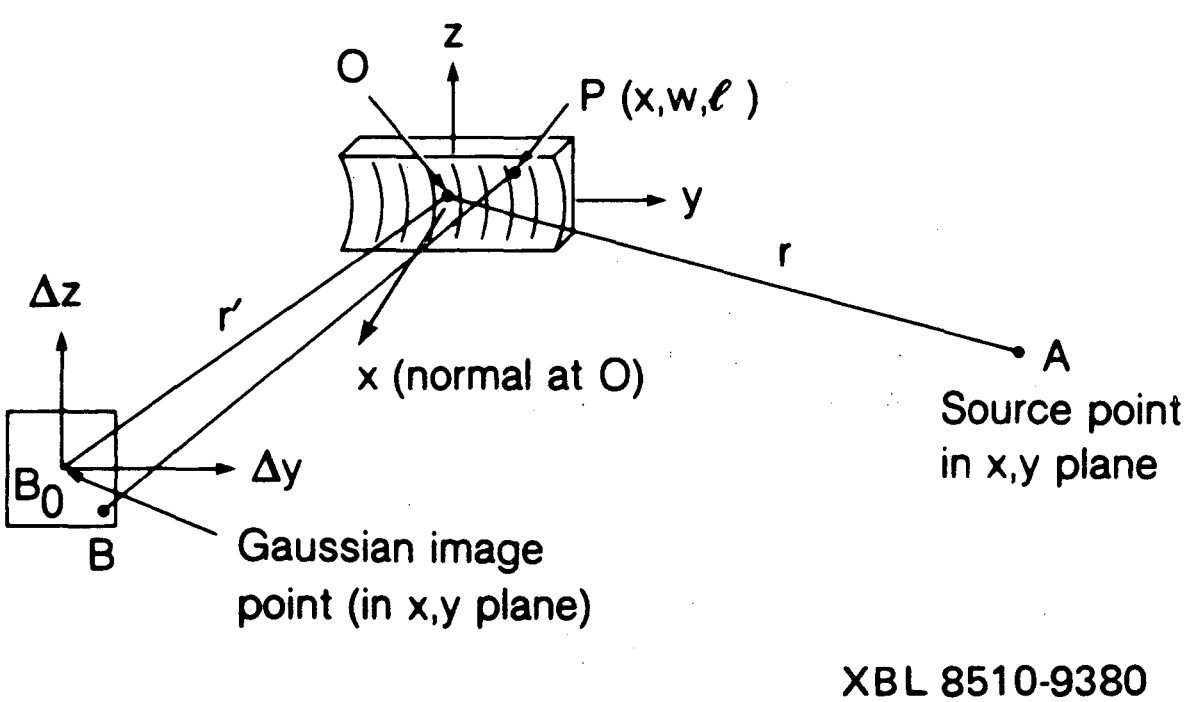

Fig. 2 Notation for analysis of diffraction by a toroidal grating

planes with spacing $d\sin\theta_B$

2.2 Fixed in and out directions

This means

$$\alpha-\beta = 2\theta = \text{constant} \qquad (4)$$

where 2θ is the included angle between the in and out directions. θ is always positive. Eliminating α between (1) and (4) gives

$$m\lambda = 2d\cos\theta\sin(\theta+\beta) \qquad (5)$$

$(\theta+\beta)$ is the angle between the diffracted ray and zero order. Thus (5) allows the possibility of a linear wavelength drive if the grating is rotated by a sine bar mechanism whose zero position (line of drive perpendicular to the sine bar) corresponds to the grating being at zero order. The wavelength scan ends at $\alpha=90°$ (positive order) or $\beta=90°$ (negative order). This happens at the so called horizon wavelength λ_H where

$$\lambda_H = 2d\cos^2\theta \qquad (m=\pm1) \qquad (6)$$

2.3 Constant incidence angle

With α constant (1) give β directly

2.4 Constant focal distance (of a plane grating)

We show later that this requires

$$\frac{\cos^2\alpha}{\cos^2\beta} = K = -\frac{r}{r'} \qquad (7)$$

Again eliminating α between (1) and (7) leads to

$$\left[\frac{m\lambda}{d} - \sin\beta\right]^2 = 1 - K(1-\sin^2\beta) \qquad (8)$$

2.5 Applications

Equations (3), (5) and (8) can readily be inverted to give β (and thence α) for any λ. The following monochromator systems used for synchrotron radiation applications are based on the above concepts

2.1 Hunter et al[1] double plane grating monochromator (PGM) Kunz[2] et al PGM

2.2 Mijake et al[3] PGM, West et al[4] PGM, Howells et al (PGM)[5], Eberhardt et al[6] (PGM), all grazing incidence toroidal grating monochromators (TGM's)[7], Seya-Namioka[8,9], most aberration reduced holographic spherical grating devices.

2.3 Essentially all spectrographs, Grasshopper monochromator[10]

2.4 Petersen[11]: SX700 PGM, Brown et al[12] UMO: PGM

3. FOCUSSING PROPERTIES OF A TOROIDAL GRATING

Consider a toroidal grating with radii R(major) and ρ(minor) illuminated by a point source (A) in its symmetry plane. Assume ρ is chosen to correct astigmatism at some wavelength in the working range. The arrangement and notation[13] are shown in fig 2. The Gaussian (paraxial) image point is B_0. The ray via the point $P(x,w,\ell)$ on the grating surface arrives in the Gaussian image plane at B. When P is at or near the grating pole (0) the paraxial approximation is good and the rays unite at B_0. As P gets further away from 0, the paraxial approximation begins to fail and aberrations become significant resulting in the point B moving away from B_0 in a way which depends on the co-ordinates w,ℓ of P. We characterise this situation by calculating the optical path function[14] (F) in the form of a power series in w,ℓ as follows[13]

$$F = F_{00} + wF_{01} + 1/2w^2F_{20} + 1/2\ell^2F_{02} + 1/2w^3F_{30} + 1/2w\ell^2F_{12} + 1/8w^4F_{40} + \ldots \qquad (9)$$

where

$$F_{00} = r + r' \qquad (9a)$$

$$F_{01} = \frac{m\lambda}{d} - \sin\alpha - \sin\beta \qquad \text{Grating equation} \qquad (9b)$$

$$F_{20} = \sum T \qquad \text{Defocus} \qquad (9c)$$

$$F_{02} = \sum S \qquad \text{Astigmatism} \qquad (9d)$$

$$F_{30} = \sum \frac{\sin\alpha}{r} T \qquad \text{Coma} \qquad (9e)$$

$$F_{12} = \sum \frac{\sin\alpha}{r} S \qquad \text{Astigmatic Coma} \qquad (9f)$$

$$F_{40} = \sum \frac{4\sin^2\alpha}{r^2} T - \frac{T^2}{r} + \frac{S}{R^2} \qquad \text{Spherical aberration} \qquad (9g)$$

and $T = \frac{\cos^2\alpha}{r} - \frac{\cos\alpha}{R}$, $S = \frac{1}{r} - \frac{\cos\alpha}{\rho}$

The $\sum$ implies that a second expression must be added that is identical to the first except for the replacements $r \to r'$ and $\alpha \to \beta$. The condition for a focus in the plane of dispersion is from equation (9c)

$$\frac{\cos^2\alpha}{r} - \frac{\cos\alpha}{R} + \frac{\cos^2\beta}{r'} - \frac{\cos\beta}{R} = 0 \qquad (10)$$

This equation can be satisfied in various ways which we discuss below.

3.1 The Rowland Circle

Suppose we put $r = R\cos\alpha$, $r' = R\cos\beta$. This sets the two brackets

in (10) separately equal to zero and implies that A and B_0 lie on a circle of diameter R : the Rowland Circle.[15] From (9e) coma also vanishes in this case. For an astigmatism corrected toroid satisfying the Rowland condition, the remaining aberrations and hence the resolution become dominated by astigmatic coma according to (9f). If astigmatism is not corrected as for example in the spherical grating, then the expansion (8) is no longer adequate. This is because the assumption of a point source and approximately corrected astigmatism justified the omission of all terms depending on the field variables at both source and image. Without the corrected astigmatism assumption we must include terms depending on Δz in fig 2. The result of doing this is a more complicated $w\ell^2$ term[16] in (9) which turns out to give much smaller contributions to the resolution which are negligible compared to the spherical aberration. The latter therefore becomes the dominant aberration of the spherical grating Rowland mount.[17,18] From this argument it is clear that spherical gratings have better resolution than toroidal ones in all cases.

3.2 The Wadsworth mounting[19,20]

(10) is satisfied if $r = \infty$ and

$$r' = \frac{R\cos^2\beta}{\cos\alpha+\cos\beta} \qquad (11)$$

For a given α (11) defines a focal curve which is rather flat in the region of $\beta=0$ allowing a useful working region for normal incidence applications.

3.3 The plane grating

If $R = \infty$ in (10) one has

$$r' = - r \frac{\cos^2\beta}{\cos^2\alpha} \qquad (12)$$

Showing that there is a virtual image distant r' behind the grating. To have a fixed image at the exit slit one can design optics to keep r' fixed by choosing α and β values that satisfy equation (7). This is the basis of the SX700 monochromator.[11]

3.4 Approximate solutions

It has been found convenient for ultra high vacuum engineering of monochromators to have a simple rotation about a fixed axis as the only motion for scanning wavelength. In its simplest form, this

arrangement would have r and r' fixed. The configuration would be designed by choosing two wavelengths λ_1 and λ_2 for which an exact focus is desired. θ is then chosen on reflectance arguments, d on horizon arguments (equation (6)) and then the α and β values corresponding to λ_1 amd λ_2 would be found from (5) and (4). (10) then gives two linear equations to be solved for r and r'. The optimum way to choose λ_1 and λ_2 is discussed in reference 21. Refinements to this procedure are to have exit and entrance slits that move to maintain focus over a finite range and to choose a spherical grating[22] instead of a toroidal one to exploit the superior resolution of the former.

3.5 Focussing in the plane perpendicular to the dispersion plane

Failure to focus perfectly in the z direction in figure 2 indicates some cylindricity in the nominally spherical wavefront and is known as astigmatism. In the grazing incidence toroidal grating systems of interest to us astigmatism can be corrected at one wavelength by proper choice of ρ, i.e. ρ is chosen so that $F_{02} = 0$ which means

$$\rho = \frac{\cos\alpha+\cos\beta}{\frac{1}{r'}+\frac{1}{r}} \qquad (13)$$

In fact, when $|\alpha| + |\beta| = \text{const}$, $(\cos\alpha + \cos\beta)$ is a slowly varying function[7] so that, in practice, a ρ value chosen according to (13) will give sufficiently good astigmatism correction over the whole range. It is this capability that has caused toroidal gratings to be preferred over spherical ones for many synchrotron radiation applications in the past few years.

4. OTHER ABERRATIONS

We do not give a detailed treatment here. References 14 and 23 give lucid general explanations. Reference 24 gives a full account with synchrotron radiation applications in mind. Fig 3 gives a feeling for the type of image one gets from toroidal grating systems. Four aberrations are visible

(i) The non-zero width in the symmetry (dispersion) plane is due to defocus(F_{20})

(ii) The large curvature to the right is due to astigmatic coma (F_{12})

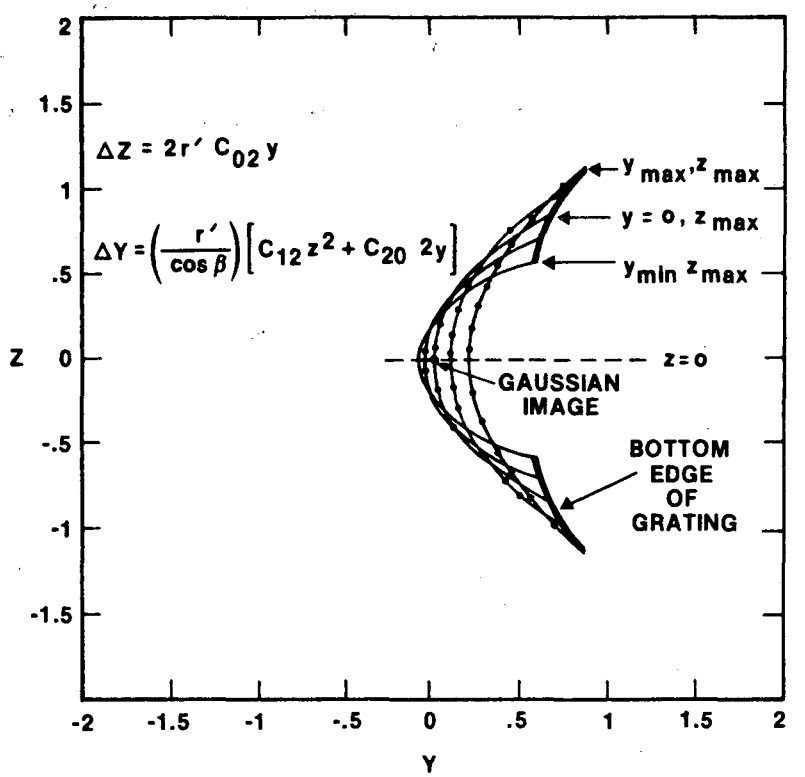

XBL 8512-5126

Fig. 3 Results of a typical ray trace for a toroidal grating. Various aberrations are evident as discussed in the text. The constants C_{12}, C_{20} are the same as F_{12}, F_{20} etc.

(iii) The weak curvature of the line labelled as due to rays from the bottom edge of the grating is due to coma (F_{30})

(iv) The non-zero height of the image is due to astigmatism.

5. QUANTITATIVE ABERRATION CALCULATIONS

The importance of the optical path function is that it enables the co-ordinates of B, ($\Delta y, \Delta z$) in fig 2 to be calculated. Furthermore it gives a decomposition of the displacements ($\Delta y, \Delta z$) into contributions Δy_{ij}, Δz_{ij} from the various aberrations. Thus

$$\Delta y_{ij} = \frac{r'}{\cos\beta} \frac{\partial F_{ij}}{\partial w} \tag{14}$$

$$\Delta z_{ij} = r' \frac{\partial F_{ij}}{\partial \ell} \tag{15}$$

$$\Delta y = \sum_{ij} \Delta y_{ij} \equiv \frac{r'}{\cos\beta} \frac{\partial F}{\partial w} \tag{16}$$

$$\Delta z = \sum_{ij} \Delta z_{ij} \equiv r' \frac{\partial F}{\partial \ell} . \tag{17}$$

These equations are proved except for the $\cos\beta$ factor, which is due to grazing incidence, in references 14 and 23.

Of course for monochromators the most interesting quantity to estimate is the resolution. This is easily derived from (16) as we now show.

6. DISPERSION AND RESOLUTION

By differentiating the grating equation with respect to β at constant α we find the angular dispersion

$$\left(\frac{d\lambda}{d\beta}\right)_\alpha = \frac{d\cos\beta}{m} \tag{18}$$

Let us now define a co-ordinate q in the plane of the exit slit in direction Δy (fig 2). Apparently $dq = r'd\beta$. So using this and (18) we obtain the reciprocal linear dispersion

$$\left(\frac{d\lambda}{dq}\right)_\alpha = \frac{d\cos\beta}{mr'} \equiv \frac{10^{-3}d(\text{Å})\cos\beta}{mr'(m)} \text{ Å/mm} \tag{19}$$

For the Rowland case $\cos\beta/r' = 1/R$ in (19) giving a constant value for the reciprocal linear dispersion.

If we consider a monochromatic source ($d\lambda=0$) then the grating equation gives us $\cos\alpha d\alpha = -\cos\beta d\beta$. If the source and image

sizes are s and s' respectively then $d\alpha = s/r$, $d\beta = s'/r'$ and we get an expression for the magnification $M(\lambda) = s/s'$

$$M(\lambda) = \frac{\cos\alpha\ r'}{\cos\beta\ r} \tag{20}$$

We see that $M(\lambda) = 1$ for all λ for the Rowland case. Notice that $M(0) = r'/r$, as expected, and $M(\lambda) > M(0)$ for negative order and $M(\lambda) < M(0)$ for positive order.

Suppose we are imaging a monochromatic source with zero width entrance and exit slits. This is possible in the geometrical optics view of imaging. Suppose the source moves a small distance s. Then we have $d\alpha = s/r$. In addition from (1)

$$\left(\frac{d\lambda}{d\alpha}\right)_\beta = \frac{d\cos\alpha}{m}$$

So

$$\Delta\lambda_s = \frac{sd\cos\alpha}{mr} \tag{21}$$

This is the slit width (or source size) contribution to the resolution. By a similar argument the exit slit contributes an amount

$$\Delta\lambda_{s'} = \frac{s'd\ \cos\beta}{mr'} \tag{22}$$

We see that $\Delta\lambda_s = sd/mR$ for the Rowland case and similarly for $\Delta\lambda_{s'}$. The aberrations contribute an amount which for each ray is given by setting s' in (22) equal to Δy so that

$$\Delta\lambda_A = \frac{\Delta y d\cos\beta}{mr'} = \frac{d}{m}\frac{\partial F}{\partial y} \tag{23}$$

It is unusual in grazing incidence systems to be close to the diffraction limit. However, with synchrotron sources planned that produce diffraction limited beams well into the VUV plus the increasing use of the partial coherence properties of synchrotron radiation for coherent imaging experiments we must consider it. It is proved, for example, in reference (14) that the diffraction limited resolution $\Delta\lambda_D$ of a grating with N grooves is given by

$$\Delta\lambda_D = \lambda/mN \tag{24}$$

In the event that the optical system of a monochromator is imperfect this will add a further contribution to the resolution. Suppose the line spread function due to imperfections is of width h then the resolution contribution will be

$$\Delta\lambda_{LSF} = \frac{hd\cos\beta}{mr'} \tag{25}$$

Equations (21) - (25) give the five main contributions to the resolution of a monochromator. The actual resolution function is obtained by convolving the five resolution functions together. The width of the overall resolution function is therefore usually estimated by combining the five widths quadratically.

7. PHASE SPACE ACCEPTANCE

Suppose the grating in fig 2 has width w_o. The beam of light illuminating the grating has emittance ε given by

$$\varepsilon = \frac{w_o \cos\alpha}{r} \cdot s$$

Setting $w_o = Nd$ and expressing this from the view point of the illuminating beam,

$$A(\Delta\lambda_s) = N\ \Delta\lambda_s/4 \qquad (26)$$

where $A(\Delta\lambda_s)$ is the phase space acceptance. If $\Delta\lambda_s$ is in Å then A is in Å.radians. The 1/4 comes from our wish to be compatible with accelerator physics and define phase space in terms of half widths and angles.

This is an important equation. It shows firstly that the acceptance varies with the slit-width-limited resolution. It also shows how to compare the phase space of the synchrotron source with the phase space of the monochromator. We know that if the emittance of the photon beam from the source is larger than $A(\Delta\lambda_s)$ by some factor F, then one must sacrifice a factor F in flux to work at that resolution. We show in figure 4 a plot which in this authors opinion is the proper way to show the resolution - flux trade-offs of a particular monochromator working with a particular source and is also the proper way to compare the characteristics of competing monochromator designs.

The monochromator whose data are plotted in fig 4 is under construction at Lawrence Berkeley Laboratory. It is a 55 meter, Rowland Circle device using a water cooled spherical grating in a conventional TGM mount. The included angle (2θ) is 174° and the overall length 6 meters.

All the curves refer to the use of full aperture for the 180 mm wide, 1100 ℓ/mm grating. The ultimate resolution displayed is the spherical aberration limit. The actual resolution should equal the spherical aberration limit in the region 15-25Å and be less good

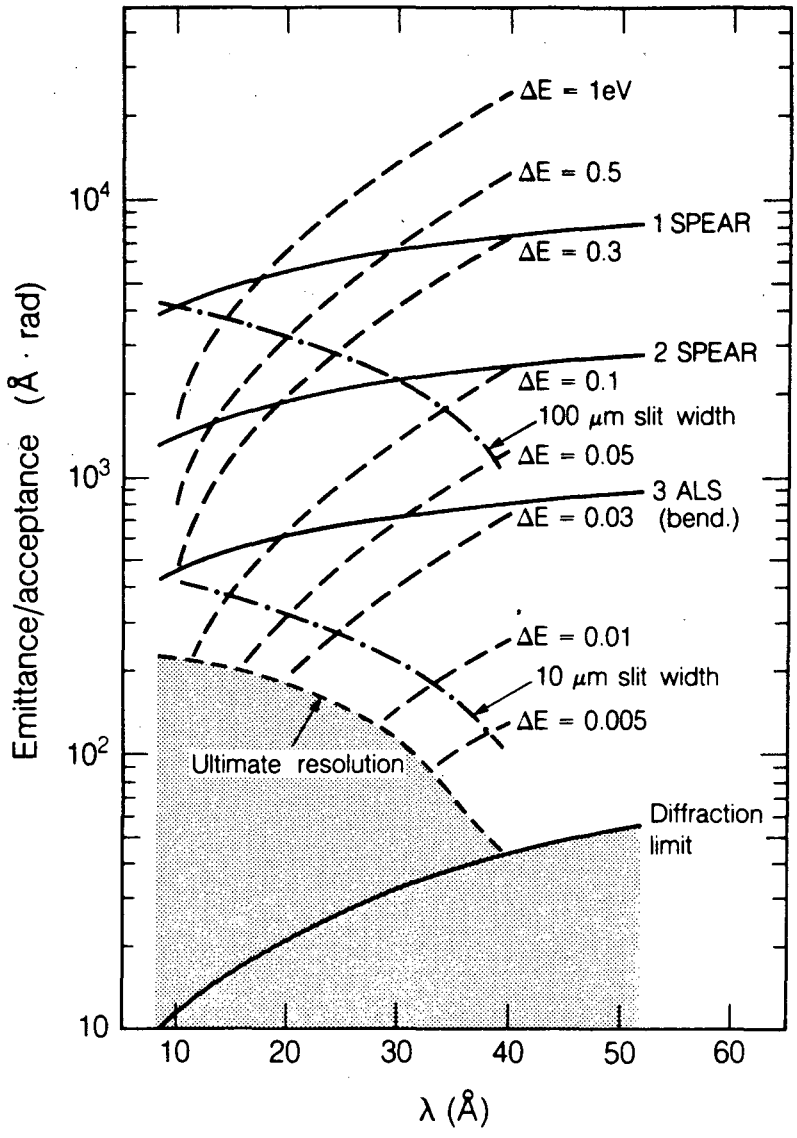

XBL 8511-12215

Fig. 4 Comparison of the source emittances and the acceptance of the spherical grating monochromator under different operation modes. The solid curves 1, 2, refer to SPEAR (54 pole wiggler for 3 GeV and 1.3 Tesla at normal operation (1), and with the low emittance upgrade (2), curve 3 refers to an ALS bending magnet. The long-dashed curves show the acceptance when the entrance slit of the monochromator is set for constant energy resolution ΔE. Usually a monochromator is operated with fixed entrance slit width which results in the dash-dotted acceptance curves. Both sets of curves are based on the assumption that the resolution is slit width limited and that the grating is always at full aperture (18cm width). The ultimate resolution of the monochromator, which is given mostly by the spherical aberration (short-dashed curve) and partly by the diffraction limit, is indicated by the shaded area. This figure shows which resolution can be achieved and how much of the incident flux is therefore lost.

outside that. The figure tolerance required is about 1μR which should be achieved for a spherical surface, however, achieving an adequate finish may be quite challenging. The most difficult practical problem is mechanical stability over the 6 meter length.

From (26) we see that the resolution-luminosity product (RLP) (or more properly the resolving power-phase space acceptance product) is given by $N\lambda/4$ in the slit-width-limited regime. The resolution luminosity product is intended to be a figure of merit to compare competing designs so if we always work in the slit-width-limited regime then the design with the largest N wins. A more useful way to interpret the resolution-luminosity product is as the ultimate resolving power ($\lambda/\Delta\lambda_u$) times $A(\Delta\lambda_s)$ so we get

$$RLP = N\lambda \frac{\Delta\lambda_s}{\Delta\lambda_u} \tag{27}$$

which is a function of λ and $\Delta\lambda_s$ which can be plotted for given instruments for comparison purposes.

REFERENCES

1. W.R. Hunter, R.T. Williams, J.C. Rife, J.P. Kirkland, and M.N. Kabler, Nucl. Instrum. Meth. 195m 141(1982), and W.R. Hunter, Proc. SPIE 315, 19(1981).
2. H. Dietrich and C. Kunz, Rev. Sci. Instrum. 43, 434(1972), and C. Kunz, R. Haensel, and B. Sonntag, J. Opt. Soc. Am. 58, 1415(1968).
3. K.P. Miyake, R. Kato, and H. Yamashita, Sci. Light 18, 39(1969).
4. J.B. West, K. Codling, and G.V. Marr, J. Phys. E7, 137(1974).
5. M.R. Howells, D. Norman, G.P. Williams, and J.B. West, J. Phys E 11, 199(1978), and M.R. Howells, Nucl. Instrum. Meth. 177, 127(1980).
6. W. Eberhardt, G. Kallsollen, and C. Kunz, Nucl. Instrum. Meth 152, 81(1978).
7. R.P. Madden and D.L. Ederer, (abstract), J. Opt. Soc. Am. 62, 722(1972), and D. Lepere, (in French), Nouvelle Revue Optique 6, 173(1975).
8. M. Seya, Sci. Light 2, 8(1952), and T. Namioka, Sci. Light 3, 15(1954).
9. For a review, see T. Namioka, M. Seya, and H. Noda, Jpn. J. Appl. Phys. 15, 1181(1976).

10. F.C. Brown, R.Z. Bachrach, and N. Lien, Nucl. Instrum. Meth. 152, 73(1978).

11. H. Petersen, Opt. Commun. 40, 402(1982).

12. F.C. Brown and S.L. Hulbert, Nucl. Instrum. Meth. Phys. Res. 222, 42(1984).

13. H. Haber, J. Opt. Soc. Am. 40, 153(1950). The general theory of the grating [H. Noda, T. Namioka, and M. Seya, J. Opt. Soc. Am. 64, 1031(1974)] is applicable to the toroid with a_{ij} values as follows: $a_{20} = 1/(2R)$, $a_{02} = 1/(2\rho)$, $a_{40} = 1/(8R^2)$, $a_{22} = 1/(4R^2\rho)$, $a_{04} = 1/(8\rho^3)$, all other $a_{ij} = 0$ for $i + j \leqslant 4$.

14. M. Born and E. Wolf, "Principles of Optics", (Pergamon, Oxford, 1983, Chapter 5 especially equation 10 in 5.2. Note these authors use the term "Characteristic function" instead of "Optical path function".

15. H.A. Rowland Phil. Mag. 16, 197 and 210(1883)

16. W.T. Welford in "Progress in Optics", E. Wolf (ed) volume 4(1965) Chapter VI, especially equations (15)-(17)

17. J.E. Mack, J.R. Stehn and B. Edlen, J. Opt. Soc. Am. 22, 245(1932)

18. I.S. Bowen J. Opt. Soc. Am. 23, 313(1933)

19. F.L.O. Wadsworth, Astrophys. J. 3, 47(1896)

20. M.R. Howells Nucl. Inst. Meth. 195, 215(1982)

21. W.R. McKinney and M.R. Howells, Nucl. Inst. Meth. 172, 149(1980) and C.T. Chen, E.W. Plummer and M.R. Howells, Nucl. Inst. Meth. 222, 103(1984)

22. W.A. Rense and T. Violett J. Opt. Soc. Am. 49, 139(1959)

23. W.A. Welford, "Geometrical Optics", (North Holland, Amsterdam, 1962)

24. R.L. Johnson in "Handbook on Synchrotron Radiation" Volume 1A, E-E Koch (ed) (North Holland, Amsterdam 1983)

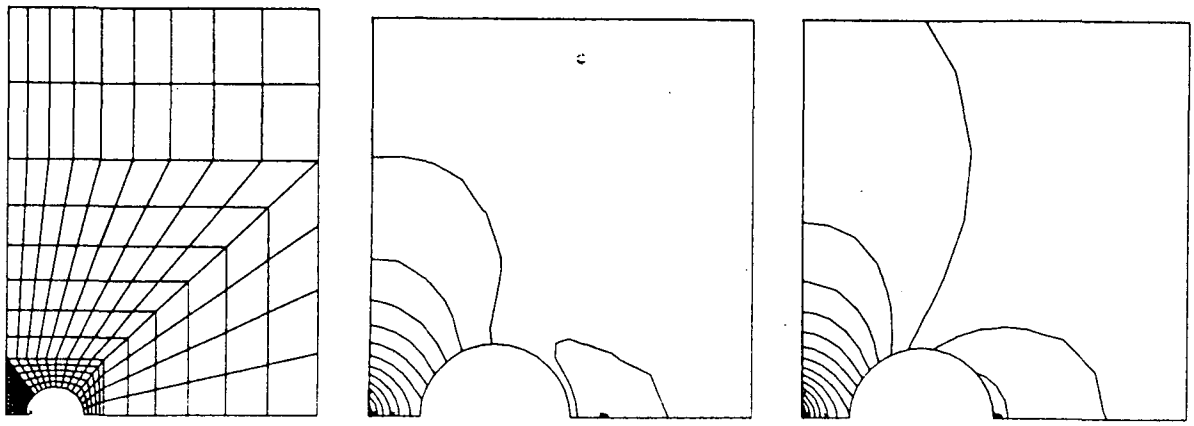

Fig 6. Example of a two dimensional finite element calculation. Left picture shows the mesh of points describing a 6 mm diameter water channel in a copper alloy mirror, at a distance 2 mm from the optical surface. An approximately gaussian power load with σ = .85 mm, peak power density 5 W/mm² is applied symmetrically. Center picture shows the isothermals calculated by the finite element program ANSYS at 2°C intervals. The hottest point on the optical surface is the center point at 72.5°C. The water surface is at 58°C on the hot side, 39°C on the cold. Right hand picture shows the stress contours (Von Mises equivalent) at 4x10⁶ Pa intervals. Maximum stress occurs at the center and is 9.12x10⁷ Pa(≡ 13200 psi), hence the use of the special copper alloy: Glidcop (see reference 49)

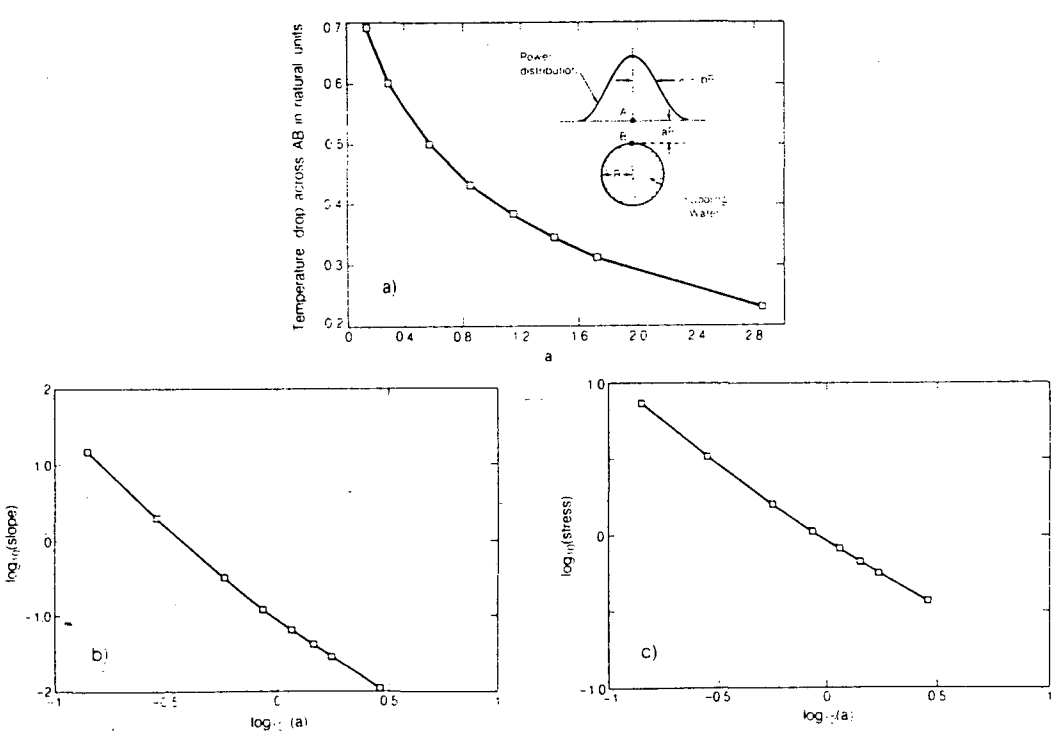

Fig 7. Plots of (a) ΔT_{AB}, (b) maximum slope error and (c) maximum stress as a function of the parameter a with parameter b = 0.243 (see inset diagram). All these quantities are expressed in the natural units defined in the text.

This report was done with support from the Department of Energy. Any conclusions or opinions expressed in this report represent solely those of the author(s) and not necessarily those of The Regents of the University of California, the Lawrence Berkeley Laboratory or the Department of Energy.

Reference to a company or product name does not imply approval or recommendation of the product by the University of California or the U.S. Department of Energy to the exclusion of others that may be suitable.

LAWRENCE BERKELEY LABORATORY
TECHNICAL INFORMATION DEPARTMENT
UNIVERSITY OF CALIFORNIA
BERKELEY, CALIFORNIA 94720